MARS CLIMATE DATABASE v3.0
DETAILED DESIGN DOCUMENT

(ESTEC Contract 11369/95/NL/JG)

S. R. Lewis, M. Collins (AOPP) and F. Forget (LMD)

April 2001

Abstract

This is the Detailed Design Document for version 3.0 of the Mars Climate Database (MCD) and replaces previous versions which described version 1.0, 2.0 and 2.3. Version 3.0 of the MCD incorporates several improvements, outlined in this document. This document reproduces and updates material from Collins and Lewis (1997b), where it is still relevant, as well as adding sections on the new features. The MCD User Manual (Lewis et al., 2001a) should be consulted for more information on how to compile and use the software supplied with the database to access the data.

Contents

1 Introduction

The Mars Climate Database (MCD) is a database of atmospheric statistics compiled from state-of-the-art General Circulation Model (GCM) simulations of the Martian atmosphere. The models used to compile the statistics have been extensively validated using available observational data and represent the current best knowledge of the state of the Martian atmosphere given the observations and the physical laws which govern the atmospheric circulation and surface conditions on the planet.

This document provides the user of the MCD with a detailed description of the database structure and of the access software. Descriptions of the models and of the validation procedure are available in other documents relating to the project.

The MCD can also be accessed in a variety of data formats using the World Wide Web at `http://www.lmd.jussieu.fr/mars.html`.

2 Differences Between Version 3.0 and Previous Versions of the MCD

- The main differences between version 3.0 and 2.3 are related to the content of the database files as a result in particular of improvements made in the models used to compile the database :
  1. The models and the derived database cover a greater range of altitude, from 0 to 120 km, with 32 layers in the vertical.
  2. The models use improved surface properties data from the Mars Global Surveyor spacecraft, including the accurate topography from the Mars Observer Laser Altimeter and the new thermal inertia map from the Thermal Emission Spectrometer.
  3. The database includes a more realistic dust scenario to describe the distribution of airborne dust in the atmosphere based on recent observations from Mars Global Surveyor.
  4. The database now includes solar and thermal infrared radiative fluxes at the surface and at the top of the atmosphere.
  5. The horizontal resolution of the database has changed to $5^\circ \times 5^\circ$.
- The main difference between version 2.3 and 2.0 was the use of the main subroutine ATMEMCD which computes meteorological variables from Mars Climate Database (MCD). This new subroutine has been especially designed for atmospheric trajectory computation, and is useful for other purposes.

- The principal difference between version 2.0 and 1.0 of the MCD was that the large-scale variability model now makes use of two-dimensional, multivariate Empirical Orthogonal Functions (EOFs), which describe correlations in the

model variability as a function of both height and longitude (rather than solely of height as in version 1.0). These are described in the Detailed Design Document which accompanies this report. The 2-D EOFs allow realistic variability to be modelled for trajectories which span a range of longitudes. As in version 1.0, EOFs are stored for a range of latitude bands, but instead of retaining 6 1-D EOFs at each horizontal location for each of 12 seasons, now 72 2-D EOFs are stored for each latitude band and their amplitude is modelled by a set of principal components tabulated once per day (669 times) throughout the model Mars year. This procedure is no more costly to the end-user in terms of either disk storage or CPU time, but gives a much improved description of the variability as a function of both space and time and a larger variance capture.

There have also been numerous small improvements and error corrections to the climate database access software since version 1.0 was released, which are now all incorporated into version 3.0.

3 Database Structure

3.1 The Data Retrieval and Storage (DRS) System

The data in the MCD are written using the Data Retrieval and Storage (DRS) library developed for the Program for (Terrestrial) Climate Model Diagnosis and Intercomparison (PCMDI). The library, available from the Lawrence Livermore National Laboratory World Wide Web server (`http://www-pcmdi.llnl.gov/drach/DRS.html`) is provided on CDROM#1 along with the database.

DRS was developed as part of the Atmospheric Model Intercomparison Project (AMIP) to facilitate the transfer of data between platforms which may have different representations of floating point numbers. It also has a number of features to enable easy updating of model history files both in terms of temporal extension and in the addition of new diagnostic variables. It can be read by many data handling and graphical packages such as GrADS.

One of the advantages of the DRS data format which has been used for the database is that the actual byte ordering of the data (often called "big endian") is independent of the type of machine that is used to read and write the data, provided the DRS library routines are used. Hence the binary database files are portable and can be read on any type of machine with programs which make use of DRS subroutines. When accessing the DRS files using GrADS from a "big endian" machine (such as a Sun or HP) this also presents no problem. However, if GrADS is run on a "little endian" machine (such as a DEC or IBM PC) it is still straightforward to read the database files owing to the presence of a record, `options big_endian`, near the head of the `.ctl` file corresponding to the `.dat` file which is being read. This record causes GrADS

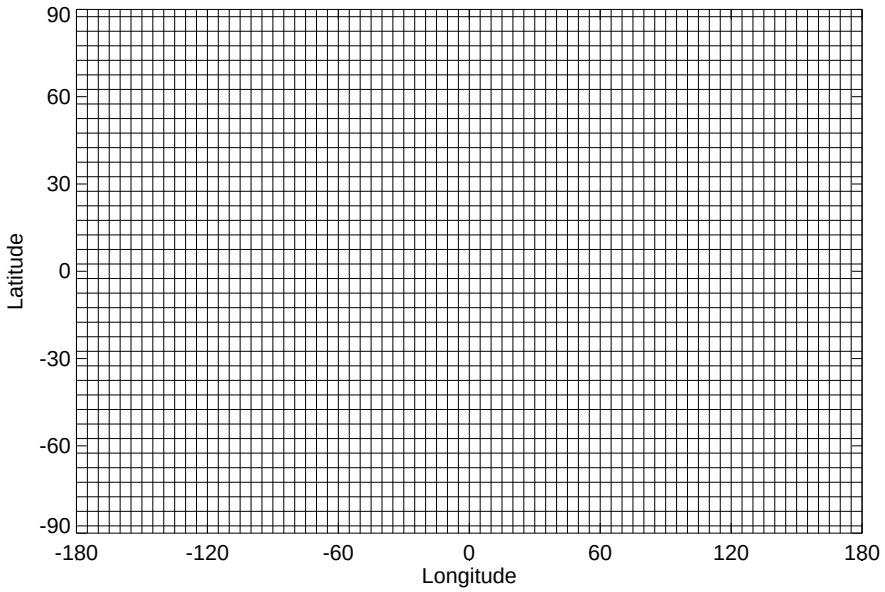

Figure 1: The database horizontal grid of 72 longitude and 36 latitude points.

to swap the byte order if the data are read on a "little endian" machine but is effectively ignored on a "big endian" machine. Hence, the binary data files for the Mars Climate Database are portable between any type of computer, whatever the details of byte ordering, provided that one of the three access methods (the MCDGM interface, program subroutines calling the DRS library, or GrADS with the `.ctl` files supplied) described in the User Manual is adopted. Files ending in `.dat` can be transferred between machines in binary format and files ending in `.ctl` can be transferred as plain text; no further conversion is necessary.

3.2 Database Grid Structure

3.2.1 Horizontal Structure

Variables in the database[1] are written on an equally spaced horizontal grid of 72 longitude points numbered from 0° to 355.° East in steps of 5° and 36 latitude points numbered from -87.5° to 87.5° in steps of 5° (latitudes South of the equator are indicated by negative numbers). See Figures 1 and 2.

[1]The general circulation models used to compile the database were run with a higher resolution of $3.75^\circ \times 3.75^\circ$ (grid 96×48). For simplicity and to reduce the size of the database, the data are stored on $5^\circ \times 5^\circ$ grid.

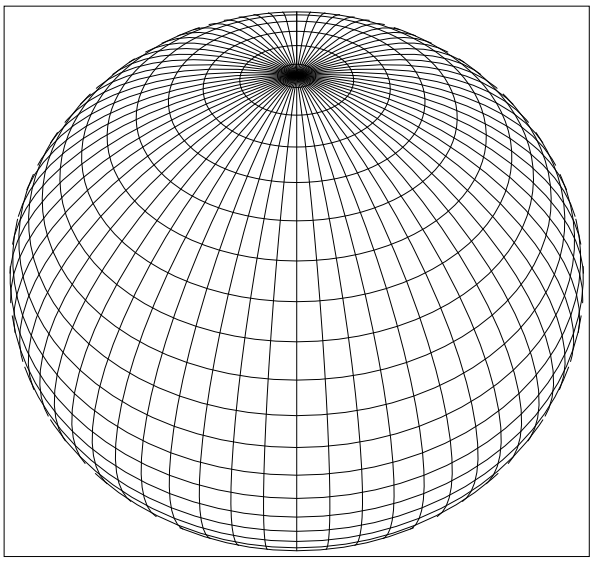

Figure 2: “Satellite” view (above latitude 60N) of the database grid illustrating the higher density toward the poles

3.2.2 Vertical Structure

The database vertical coordinate is defined as

$$\sigma = \frac{p}{p_s} \tag{1}$$

where p is the atmospheric pressure and p_s is the surface pressure. Thus σ is 1 at the surface, 0 at infinite height and the σ levels follow the model orography. The sigma levels are arranged as in Table 1 and illustrated in Figure 3.

Layer	σ	**Approximate Height** for mean Mars atmosphere temperatures	*pseudo-height in* `name_a.ctl` *files (based on* $-10\ln(\sigma)$ *)*
1	0.999500	5 m	*5.00 m*
2	0.998001	20 m	*20.0 m*
3	0.995013	50 m	*50.0 m*
4	0.989086	115 m	*109.7 m*
5	0.977443	240 m	*228.15 m*
6	0.955004	490 m	*460.40 m*
7	0.913289	980 m	*907.03 m*
8	0.840606	1.8 km	*1.736 km*
9	0.726845	3.4 km	*3.190 km*
10	0.574642	7 km	*5.540 km*
11	0.407472	9.6 km	*8.978 km*
12	0.258882	14.2 km	*13.51 km*
13	0.150070	19.5 km	*18.97 km*
14	0.081573	25 km	*25.06 km*
15	0.042627	31 km	*31.55 km*
16	0.021789	37 km	*38.26 km*
17	0.011008	43 km	*45.09 km*
18	$5.52812\ 10^{-3}$	48 km	*51.98 km*
19	$2.76764\ 10^{-3}$	54 km	*58.90 km*
20	$1.38349\ 10^{-3}$	60 km	*65.83 km*
21	$6.91042\ 10^{-4}$	65 km	*72.77 km*
22	$3.45038\ 10^{-4}$	71 km	*79.72 km*
23	$1.72245\ 10^{-4}$	77 km	*86.67 km*
24	$8.59773\ 10^{-5}$	82 km	*93.61 km*
25	$4.29142\ 10^{-5}$	87 km	*100.56 km*
26	$2.14194\ 10^{-5}$	92 km	*107.51 km*
27	$1.06907\ 10^{-5}$	97 km	*114.46 km*
28	$5.33590\ 10^{-6}$	101 km	*121.41 km*
29	$2.66320\ 10^{-6}$	106 km	*128.36 km*
30	$1.32920\ 10^{-6}$	110 km	*135.31 km*
31	$6.63400\ 10^{-7}$	114 km	*142.26 km*
32	$2.20900\ 10^{-7}$	120 km	*153.26 km*

Table 1: Database σ levels and approximate heights above the local surface. Note that the pseudo-height is based on a 10km scale height and is particularly inaccurate in the upper atmosphere above 80 km because of the low temperatures and small scale height there.

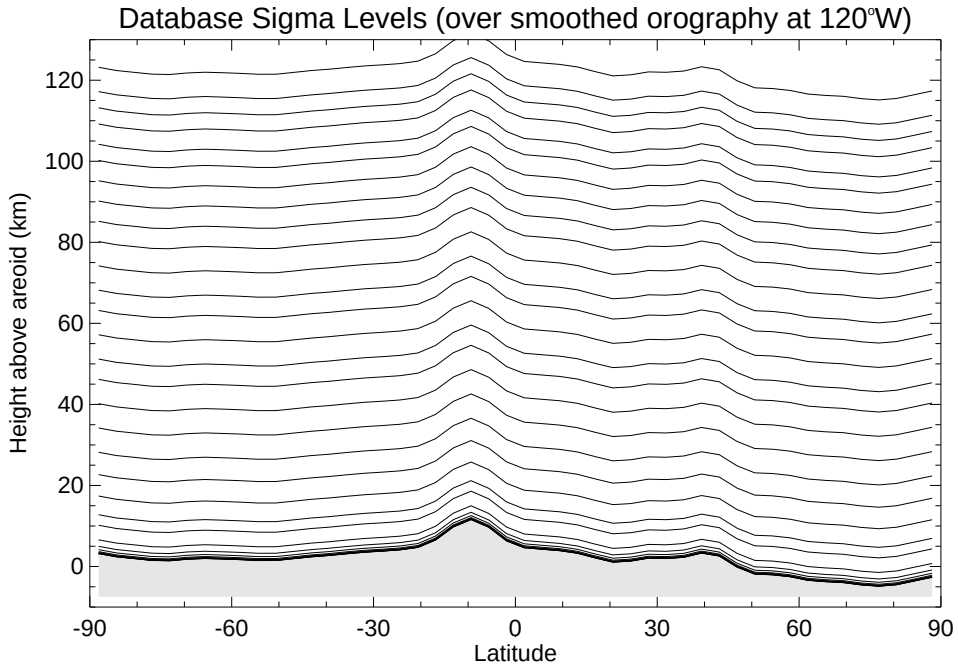

Figure 3: The database σ levels modulated by the orography at 120^{o}W. The height shown here were obtained from the hydrostatic equation assuming a constant average temperature profile.

3.2.3 Temporal Structure

Data are stored in the database 12 times per Martian day using universal time (or "prime meridian time" : local time at 0° longitude), not local time. At database time level 1 the universal time is 12pm = 0am (given that the Martian day is 24 "hours" long). Hence at 90° longitude the local time is 6am, at 180° it is 12am etc. At time level 2 the local time at 0° is 2am, etc.. All times are True Solar Times, not Mean Solar Time.

Database time level (`iut` = 1,2,... 12) can be computed from local time (0...24.) and East longitude (deg) using the following FORTRAN command:

```
iut=mod(nint(-longitude/30.+localtime/2.+12.),12)+1
```

3.3 Database File Structure

3.3.1 Documentation Files

In the `docs` directory, the following documentation Files are available:

- User Manual (`user_manual.ps` or `.pdf`) of the database V3.0
- Detailed Design Document (`detailed_design.ps` or `.pdf`) of the database V3.0
- Programmer's guide for the `atmemcd` FORTRAN subroutine (`program_guide.ps`, `.pdf` or `.doc`)
- Postscript or pdf versions of the scientific reference articles Lewis et al. (1999) and Forget et al. (1999) describing the Mars climate database V1.0 and the General Circulation models used to compile it are also provided.

3.3.2 Software Files

- `emcd` This contains FORTRAN source code for the ATMEMCD subroutine, the MCDGM interface and a test program (see `ReadMe` file in the directory and the User Manual and Programming Guide) Also included is sub-directory `testcase` containing a simple tool to test the results from the software after installation.
- `drs` This contains the DRS library (with some documentation) used to read the database files.
- `grads` Some sample GrADS scripts which plot MCD data (see Lewis et al., 2001a). Descriptions of the scripts are given in the User Manual.

  The files provided include:

```
anim_tsurf.gs   map_windt.gs    section_lat.gs  zonal_tuv.gs
map_ps.gs       profile.gs      zonal_sdtuv.gs
```

3.3.3 Data Files

The MCD data are stored in various files in a central data directory `mcd/data`.

The file naming convention is as follows:

- The first 3 characters denote the dust scenario. The various scenarios are explained in an appendix to this document.

  - `mgs` indicates Mars Global Surveyor scenario data (most realistic)
  - `ds2` indicates a dust storm with optical depth 2.
  - `ds5` indicates a dust storm with optical depth 5.
  - `low` indicates low dust data.
  - `vik` indicates Viking scenario data (relatively dusty)

- The next 3 characters indicate the season number. The northern hemisphere spring equinox is at $L_S = 0°$, with northern summer solstice at $L_S = 90°$, autumn equinox at $L_S = 180°$ and winter solstice at $L_S = 270°$.
  - `s01` is season 1, $L_S = 0° - 30°$.
  - `s02` is season 2, $L_S = 30° - 60°$.
  - `s03` is season 3, $L_S = 60° - 90°$.
  - `s04` is season 4, $L_S = 90° - 120°$.
  - `s05` is season 5, $L_S = 120° - 150°$.
  - `s06` is season 6, $L_S = 150° - 180°$.
  - `s07` is season 7, $L_S = 180° - 210°$.
  - `s08` is season 8, $L_S = 210° - 240°$.
  - `s09` is season 9, $L_S = 240° - 270°$.
  - `s10` is season 10, $L_S = 270° - 300°$.
  - `s11` is season 11, $L_S = 300° - 330°$.
  - `s12` is season 12, $L_S = 330° - 360°$.
  - `all` indicates that the file contains data for the whole year, e.g. the Empirical Orthogonal Function (EOF) data for the large-scale variability model.

- The next 2 characters indicate the type of data in the file.
  - `me` indicates mean data.
  - `sd` indicates standard deviation data.
  - `eo` indicates EOF data.

- The last 4 characters (the filename extension) indicate the type of file.
  - `.dat` is a DRS data file.
  - `.dic` is a DRS dictionary file.
  - `.ctl` is a GrADS descriptor file in $\sigma = p/p_s$ coordinate
  - `_a.ctl` is a GrADS descriptor file in pseudo-altitude $z = -10 \ln(p/p_s)$

Hence the file `mcd/data/viks04me.dat` contains mean data for the Viking dust scenario for season 4.

Mean variable	symbol	units	2-D or 3-D
CO_2 ice cover	co2ice	kg m^{-2}	2-D
Surface emissivity	emis	none	2-D
Surface temperature	tsurf	K	2-D
Surface pressure	ps	Pa	2-D
LW (thermal IR) radiative flux to surface	fluxsurf_lw	W m^{-2}	2-D
SW (solar) radiative flux to surface	fluxsurf_sw	W m^{-2}	2-D
LW (thermal IR) radiative flux to space	fluxtop_lw	W m^{-2}	2-D
SW (solar) radiative flux to space	fluxtop_sw	W m^{-2}	2-D
Atmospheric temperature	t	K	3-D
Zonal (East-West) wind	u	m s^{-1}	3-D
Meridional (North-South) wind	v	m s^{-1}	3-D
Atmospheric density	rho	kg m^{-3}	3-D
Boundary layer eddy kinetic energy	q2	m^2 s^{-2}	3-D

Table 2: Variables stored in database mean data files.

Standard deviation	symbol	units	2-D or 3-D
CO_2 ice cover	sdco2ice	kg m^{-2}	2-D
Surface emissivity	sdemis	none	2-D
Surface temperature	sdtsurf	K	2-D
Surface pressure	sdps	Pa	2-D
Atmospheric temperature	sdt	K	3-D
Zonal (East-West) wind	sdu	m s^{-1}	3-D
Meridional (North-South) wind	sdv	m s^{-1}	3-D
Atmospheric density	sdrho	kg m^{-3}	3-D

Table 3: Variables stored in database standard deviation data files.

Mean data files (`me`) contain 12 seasonal mean values (corresponding to 12 Solar times of day) for the variables shown in Table 2 and standard deviation data files (`sd`) contain seasonal standard deviation values of the variables in Table 3.

EOF data files (`eo`) contain normalized, multi-dimensional EOFs of density, zonal wind, meridional wind, temperature and surface pressure as well as some normalization factors, eigenvalues and principal component model coefficients. It is recommended that you use the software supplied to access and exploit the data in these files.

In addition there are three files, `mountain.ctl`, `mountain.dat` and `mountain.dic` which contain maps of the topographic height on Mars, smoothed to the resolution at which it is used by the model, and sub-grid scale standard deviation of the topographic height (useful for computing gravity wave perturbations). A final data file, `cospar.dat`, contains the COSPAR reference atmospheric profile, used for some output from the MCDGM interface (see Figure 10).

4 Dust Distribution Scenarios in the MCD

This section outlines the dust distribution scenarios used for the GCM integrations which make up the Mars Climate Database. For the detailed rationale behind these choices (except for the MGS scenario developped more recently) summaries of observational evidence and more references see Forget *et al.* (1999) and Lewis *et al.* (1999).

4.1 Dust vertical distribution analytical function

For all the scenarios, the vertical distribution of dust was calculated according to the formula,

$$\frac{Q}{Q_0} = \exp\left(0.007\left(1 - \max\left[\left(\frac{p_0}{p}\right)^{(70\mathrm{km}/z_{\max})}, 1\right]\right)\right) \quad (2)$$

with p the pressure, p_0 a standard pressure (700Pa), Q and Q_0 the dust mixing ratio at the pressure levels p and p_0, and $z_{\max}$ the altitude of the top of the dust layer (where the dust mixing ratio is one thousandth of its value at p_0). This formula gives a rapid decay up to the height of the top of the dust layer and almost homogeneous dust mixing in the lower regions of the atmosphere. The function is illustrated for several different values of $z_{\max}$ in Figure 7.

In fact, Equation 2 was developed from a slightly simpler form in common use for Mars modelling, namely,

$$\frac{Q}{Q_0} = \exp\left(\nu\left(1 - \left(\frac{p_0}{p}\right)\right)\right) \quad (3)$$

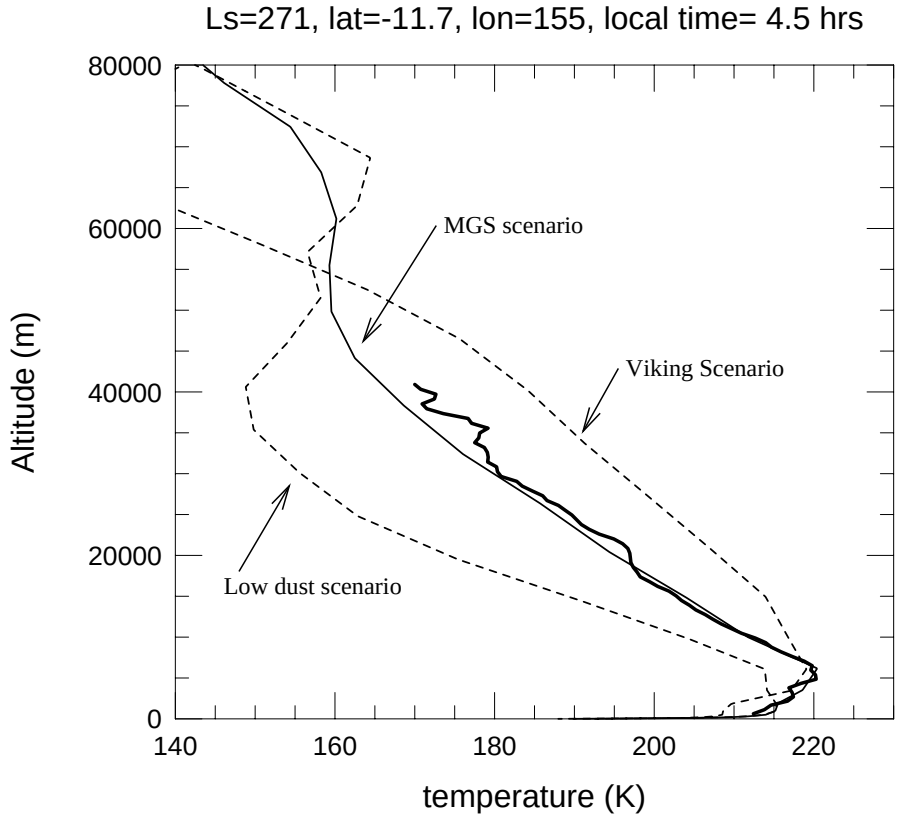

Figure 4: A typical temperature profile observed by radio-occultation (thick solid line, february 1998, $L_s = 271^o$, 11.7^oS-155^oE, local time : 4:30) compared to temperature profiles predicted by the database at the same time and location. Profiles from the "MGS" scenario are usually very close to the MGS observations, whereas the "Viking" and "low dust" scenarios yield warmer and colder temperatures profiles in the lower atmosphere, respectively.

where ν is now a parameter which determines the dust cut-off. This function is illustrated in Figure 8. Equation 3 matches Equation 2 when $z_{\max} = 70$km and $\nu = 0.007$, which were roughly the conditions under which Equation 3 was derived to model the distribution of dust at the time of the IRIS observations from Mariner 9. The reason for modifying the formula to the form in Equation 2 was that it gives much more desirable properties in terms of the total dust contained below the cut-off threshold (with a broader region of homogeneity) and the vertical gradient of the dust is not so steep near the surface, especially when the dust is mostly low in the atmosphere, compare Figure 7 with Figure 8 when $z_{\max} = 20$km and $\nu = 1.0$. While having these desirable properties the function still matches the limited available observations when the dust is high in the atmosphere.

Dust scenarios

Baseline multi-annual model integrations were carried out for the database under a total of five scenarios: **1)** A "best guess" thought to represent the moderately dusty planet Mars as observed by Mars Global Surveyor (**MGS**) without the dust storms. This scenario is recommended for those who seek ONE annual scenario to represent Mars mean climate. **2)** a very clear year with **low dust** opacity and **3)** a relatively dusty year made by generalizing the **Viking** Lander dust opacity observations to the entire planet, but with the large dust storms removed. These two additional annual scenarios are provided to bracket the possible global conditions on Mars (Figure 4) outside global dust storms which are thought be highly variable locally and from year to year. Last, **4)** a **moderate global dust storm** and **5)** an **intense global dust storm** are provided only during the period during which such global events are known to occur.

The details of the scenarios follow.

- `mgs` This is a new, standard scenario with data provided for all twelve seasons from multiannual experiments. The dust optical depth varied as a function of time (L_s) and latitude (ϕ) to match the temperature profiles (observed by radio occultation or by inverting the Thermal Emission Spectrometer data) available in september 2000. This scenario is described by 3 varying values corresponding to (1) the low latitude equatorial region (between 45^{o}N and 45^{o}S) (2) the South Polar region ($< 45^o$S) (3) The North Polar region ($> 45^o$N). The Southern and equatorial regions are affected by the increase of dust during perihelion (dust devils, local dust storms), but not the Northern regions :

$$\tau_{eq}(L_s) = 0.2 + (0.5 - 0.2)(\cos((L_s - 250^\circ)/2))^{14} \quad (4)$$
$$\tau_S(L_s) = 0.1 + (0.5 - 0.1)(cos((Ls - 250^\circ)/2))^{14} \quad (5)$$
$$\tau_N(L_s) = 0.1 \quad (6)$$

From this, he reference optical depth τ (at 700Pa) on any point of the planet is then interpolated using an hyperbolic tangent transition :

$$\tau(\phi, Ls) = \tau_N + (\tau_{eq} - \tau_N)^{0.5}(1 + \tanh((45^\circ - \phi)/10)) \quad (\phi > 0) \quad (7)$$
$$\tau(\phi, Ls) = tauS + (\tau_{eq} - \tau_S)^{0.5}(1 + \tanh((45^\circ + \phi)/10)) \quad (\phi < 0) \quad (8)$$

where ϕ is the latitude and L_s the Solar longitude of Mars.

The cut-off of the dust in the vertical also varied as a function of both time and latitude:

$$z_{\max}(L_s, \phi) = 60 + 18f - (32 + 18f)\sin(\phi)^4 - 8f * sin(\phi)^5 \quad (9)$$

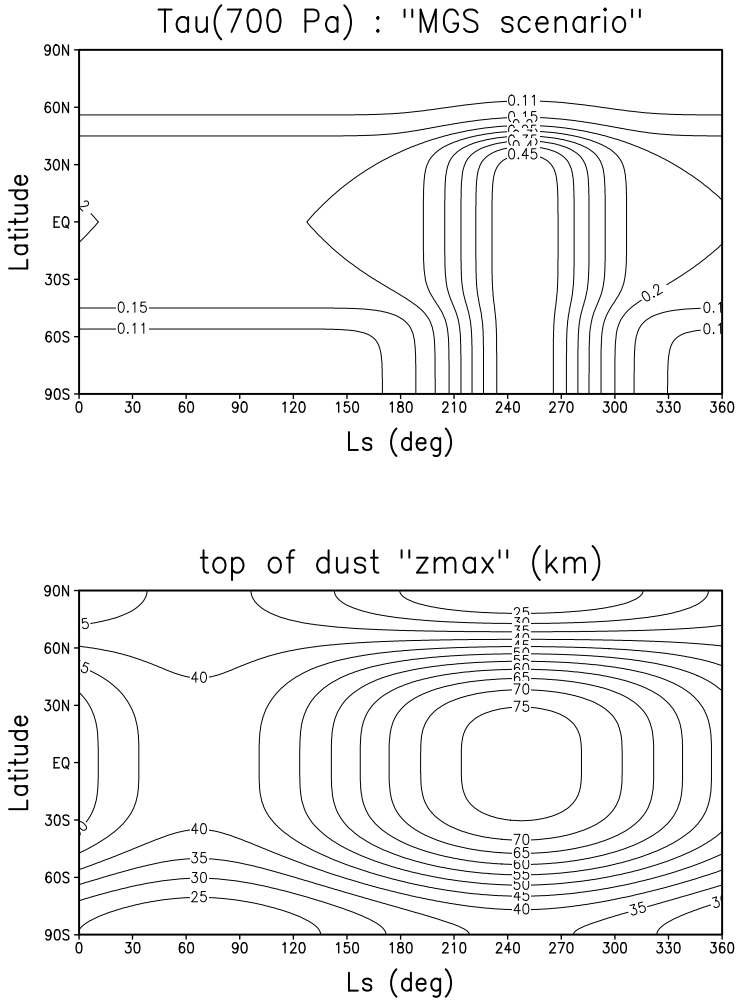

Figure 5: Variation of the reference optical depth τ at 700 Pa and the cut-off altitude of the dust distribution (see Eq. 2) as a function of season (solar longitude L_s) and latitude in the **MGS** scenario.

where $f = \sin(L_s - 160^\circ)$. The spatial and temporal evolution of τ and $z_{\max}$ are represented on Figure 5.

- `vik` The standard Viking scenario with data provided for all twelve seasons from multiannual experiments. This is the scenario orginally provided since Database Version 1.0. It is still provided here for continuity, and to provide an "upper limit" scenario for the dust content in the Martian atmosphere (outside great dust storms) The total dust optical depth for the Viking case varied as a function of time to fit the Viking Lander observations with peaks representing dust storms removed,

$$\tau(L_S) = 0.7 + 0.3\cos(L_S + 80^\circ) \tag{10}$$

where τ is the optical depth and L_S the Solar longitude of Mars. The optical depth was uniform in the horizontal for the Viking baseline run. However, the

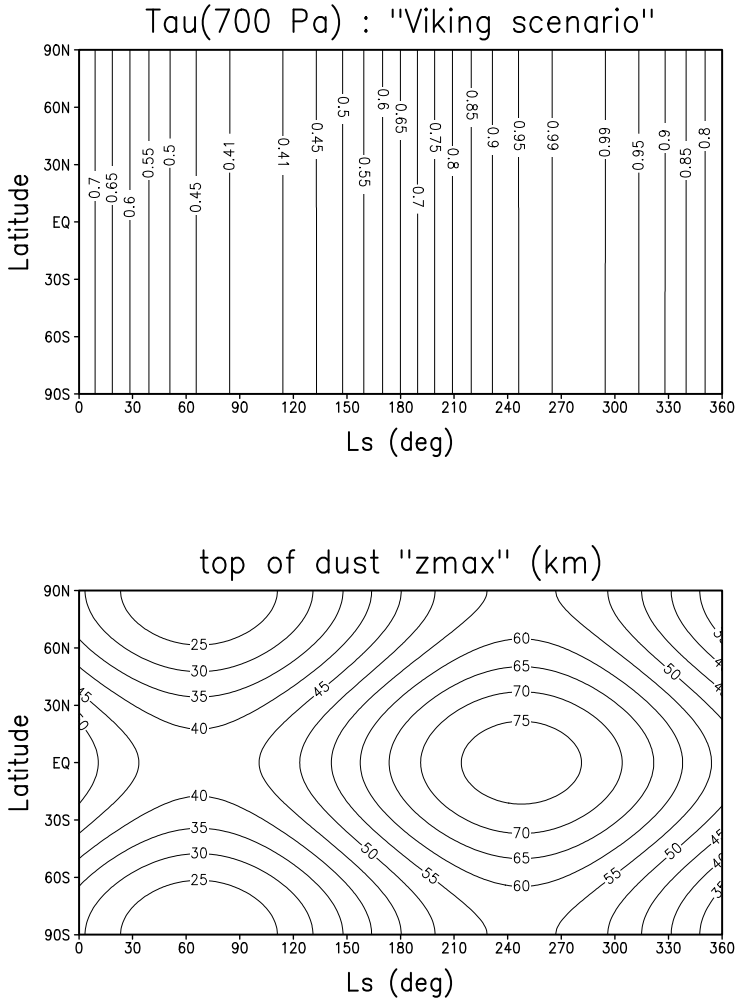

Figure 6: Variation of the reference optical depth τ at 700 Pa and the cut-off altitude of the dust distribution (see Eq. 2) as a function of season (solar longitude L_s) and latitude in the **Viking** scenario.

cut-off of the dust in the vertical varied as a function of both time and latitude,

$$z_{\max}(L_S, \phi) = \left(60 + 18\sin(L_S - 158^\circ) - 22\sin^2\phi\right) \text{ km} \qquad (11)$$

where ϕ is the latitude. $z_{\max}$ varies between 78km at the equator during the dusty seasons and 20km at the pole during the clear seasons. The spatial and temporal evolution of τ and $z_{\max}$ are represented on Figure 6.

- `low` The low dust scenario with data provided for all twelve seasons from multiannual experiments. The low dust case was conducted with a dust distribution which was invariant in latitude, longitude and time, with an optical depth of $\tau = 0.1$ and a cut-off at $z_{\max} = 30$km altitude.
- `ds2` A dust storm with maximum optical depth 2. Data from these runs are only provided for the seasons when dust storms are most likely to occur; seasons 8,

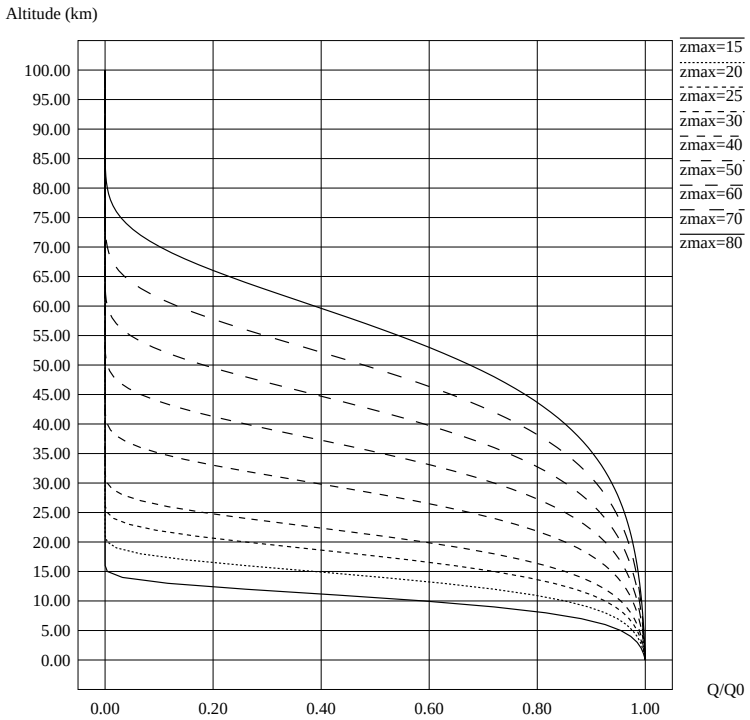

Figure 7: The variation of dust mixing ratio with height for different values of $z_{\max}$ according to the formula (Equation 2) used to compile the Mars Climate Database.

9 and 10. The dust optical depth was set to double that in the Viking scenario, Equation 10, and the vertical cut-off for the dust was modelled as in the Viking scenario, Equation 11.

- `ds5` A dust storm with maximum optical depth 5. Data from these runs are only provided for the seasons when dust storms are most likely to occur; seasons 8, 9 and 10. The dust optical depth was set to five times that in the Viking scenario, Equation 10, and the vertical cut-off for the dust was modelled as in the Viking scenario, Equation 11.

5 Variability Models

5.1 The Large-Scale Variability Model

In the MCD, data are stored in 12 seasonal bins and at 12 local times of day within each season. Although this captures the main seasonal and diurnal components of variability, any intra-seasonal or day-to-day (synoptic) variations are averaged out. Thus there is a need to simulate this variability, especially if the user wishes to produce

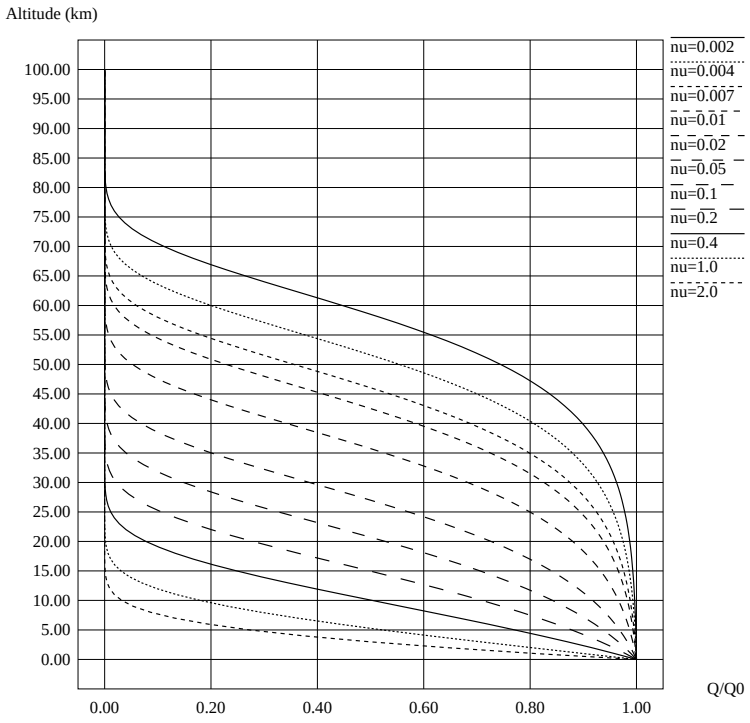

Figure 8: The variation of dust mixing ratio with height according to a formula (Equation 3) previously used in many Mars GCMs, with the ν parameter adjusted to give dust cut-offs at different heights. This function matches that in Figure 7 when $z_{\max} = 70$km and $\nu = 0.007$.

an ensemble of realizations of a variable at a particular seasonal date and local time of day which covers a realistic range of variability.

In version 1.0 of the MCD large-scale variability in a vertical profile of a meteorological variable, $D(z)$, was modelled by adding a series of functions to a mean vertical profile, $\overline{D}(z)$,

$$D(z) \; = \overline{D}(z) \; + \; \sum_{i=1}^{N} \; p_i \mathbf{e}_i(z) \tag{12}$$

where the functions $\mathbf{e}_i(z)$ are eigenvectors of the covariance matrix of all the pre-averaged profiles generated by the GCM and p_i are the amplitudes of the functions. The eigenvectors, $\mathbf{e}_i$, are often called Empirical Orthogonal Functions (EOFs) and the p_i are referred to as the Principal Components (PCs) (see, e.g. North, 1984; Mo and Ghil, 1987). The set $\{\mathbf{e}_i\}$ form an optimal linear basis such that the variance capture is high even when the truncation limit is low.

5.1.1 Horizontal Correlations

In version 1.0 only correlations in altitude between variables were considered when calculating the covariance matrix. However, in order to retain cross-correlations between different variables (zonal wind, meridional wind, temperature, surface pressure and density) all were normalized and combined together to form a set of multivariate functions. Different sets of EOFs were computed for each of the 12 seasons on a low resolution grid (20° longitude $\times$ 20° latitude) and the series (12) was truncated at $N = 6$ to reduce the demands on data storage. Even so, typically $80 - 90\%$ of the variance was retained in the version 1.0 variability model at this level of truncation.

In order to improve the model it is desirable to extend the spatial dimension to include correlations between variables in both the horizontal and the vertical. Ultimately it would be desirable to include all the longitude, latitude and vertical grid-points in the analysis. A technical point, however, must be noted here. In computing the EOFs, the eigenvalues and eigenvectors of an $N \times N$ real symmetric matrix must be found. The order, N, of the matrix depends on the number of variables and on the number of spatial points. Since the number of calculations needed to perform the eigenvector problem increases as N^3 there is a limit on the value of N that can be handled practically. The estimated CPU time and storage requirements for calculating the eigenvectors of the full problem (even on the low resolution grid with four three-dimensional and one two-dimensional variables, for which $N = 18 \times 9 \times (4 \times 25 + 1) = 16362$) is prohibitive.

We make the choice, therefore, to calculate EOFs in the two-dimensional, height-longitude plane which gives a manageable set of eigenvector problems. There is some physical basis for this choice, in that much of the variability the model must account for is in the form of baroclinic waves which, in general, propagate West to East along lines of latitude.

5.1.2 Statistical Stability and PC Modelling

In version 1.0 of the MCD we calculated separate sets of the variability EOFs for each of the 12 seasons. However, due to the relatively small number of days in each season (50–70), this can lead to poor estimation of the EOFs. Greater statistical stability can be achieved by forming the covariance matrix over the entire annual cycle, although this means that more EOFs must be retained in the series (12) in order to still capture a relatively high fraction of the variance. Fortunately this is possible as there is then no need to store the EOFs at each season. In fact the series can be extended to include 72 ($= 12 \times 6$) EOFs rather than just 6 per season with no increase in the amount of space needed to store the MCD.

This also overcomes a problem which might occur with the version 1.0 implementation of the PC modelling. If a time series of a variable was computed across a seasonal boundary there could be a discontinuity at the boundary where the quadratic fit to the intra-seasonal or trend components did not match. In the improved version 2.0 of the variability model we simply store a smooth version of each PC to represent the seasonal cycle together with a variance to represent synoptic activity. This both simplifies and improves the algorithm.

5.1.3 Calculation of EOFs and PCs

Consider a time series of longitude-pressure vectors of zonal wind, $\mathbf{u}(\phi, p, t)$, meridional wind, $\mathbf{v}(\phi, p, t)$, temperature, $\mathbf{T}(\phi, p, t)$, density, $\rho(\phi, p, t)$ and surface pressure $p^*(\phi, t)$ at M discrete time points and on L spatial points. We form a time series of vectors $\mathbf{D}(t)$, where

$$\mathbf{D}(t) \;=\; (\hat{\mathbf{u}}(\phi, p, t), \hat{\mathbf{v}}(\phi, p, t), \hat{\mathbf{T}}(\phi, p, t), \hat{p^*}(\phi, t), \hat{\rho}(\phi, p, t)) \tag{13}$$

and the hat $\hat{}$ denotes a removal of the series mean and normalization of variance operator,

$$\overline{u} \;=\; \frac{1}{ML} \sum_{m=1}^{M} \sum_{l=1}^{L} u_{ml} \tag{14}$$

$$\hat{u}_{ml} \;=\; \frac{u_{ml} - \overline{u}}{\sqrt{\frac{1}{ML} \sum_{m=1}^{M} \sum_{l=1}^{L} (u_{ml} - \overline{u})^2}} \tag{15}$$

where the m denotes time and the l denotes spatial point. Hence, with this normalization, the variance of the entire time series of $\mathbf{D}(t)$ is unity.

We then form the $(N \times N)$ covariance matrix, $\mathbf{C}$, such that

$$\mathbf{C} \;=\; \frac{1}{N} \mathbf{D}\mathbf{D}^T \tag{16}$$

where $N =$ (number of horizontal points) $\times$ (4 $\times$ number of vertical points + 1), $\mathbf{D}$ is the $(N \times M)$ matrix whose rows are the vectors $\mathbf{D}(t)$ and the superscript T indicates the transpose.

The matrix $\mathbf{C}$ is real symmetric and we can find the eigenvectors and eigenvalues and order them in decreasing eigenvalue magnitude. We note that if $\mathbf{E}_i$ is the ith eigenvector then

$$|\mathbf{E}_i| \;=\; 1 \tag{17}$$

where $|\cdot|$ is the Euclidean Norm, and

$$\sum_{i=1}^{N} \lambda_i \;=\; 1 \tag{18}$$

where λ_i is the ith eigenvalue.

The ith principal component (PC) at time m, p_{mi} is defined as

$$p_{mi} \;=\; \sum_{n=1}^{N} D_{mn} E_{ni} \;=\; \mathbf{D} \cdot \mathbf{E}_i \tag{19}$$

and we note the result

$$\frac{1}{MN} \sum_{m=1}^{M} (p_{mi})^2 \;=\; \lambda_i \tag{20}$$

Each principal component has 669 values during one year (one per day). From the PCs we calculate a 30 day running mean, ps_{mi}, and a variance departure from that mean, pv_{mi}. The modelled PC, p'_{mi}, at time m is then

$$p'_{mi} \;=\; ps_{mi} + \Phi pv_{mi} \tag{21}$$

where Φ is a normally distributed random variable with unit standard deviation.

5.1.4 Variance Capture

In version 1.0 of the variability model only 6 EOFs per location per season were retained in the series in Equation 12 to limit the amount of data storage required. Because, in the improved version, a single set of EOFs are calculated for the whole year, 72 EOFs can be retained in the series with no greater storage overhead, to give a potentially greater overall variance capture. Figure 9 shows the fraction of variance captured by retaining 72, 36, 18 and 9 EOFs at different latitudes. By retaining 36 EOFs approximately 90% or greater of the variance is captured and by retaining 72 EOFs approximately 95% or greater of the variance is captured. Including more EOFs gives relatively little increase in variance capture but increases the storage requirements considerably. Thus 72 EOFs seems to be a good compromise between variance capture and data storage.

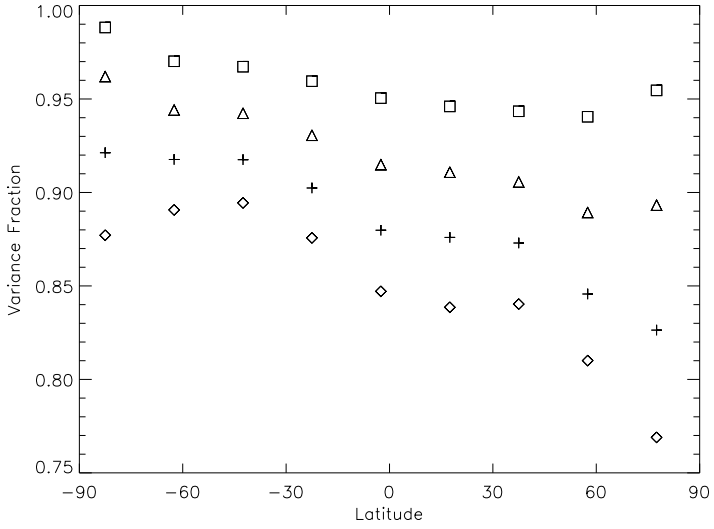

Figure 9: The fraction of variance captured by 72 EOFs (squares), 36 EOFs (triangles), 18 EOFs (plus signs) and 9 EOFs (diamonds) at different latitudes for the Viking scenario run. 72 EOFs capture more than 95% of the variance at most latitudes.

5.1.5 Examples of Cross-Sections

Density is one of the most important variables used by engineers in mission planning (e.g. when calculating entry trajectories or aerobraking manoeuvres). Hence the new variability model is illustrated using this field. Because density varies exponentially with height it is useful to compare any density profile with some 'standard' profile. Figure 10 shows the northern hemisphere COSPAR standard atmospheric density profile from the surface to approximately 90 km. All density profiles are referenced to this profile by expressing the density as a percentage difference, d, from the COSPAR profile. i.e.

$$d \; = \; 100 \times \frac{\rho_{COSPAR} - \rho}{\rho_{COSPAR}} \tag{22}$$

Figure 11 shows a selection of instantaneous longitude-height fields of density (referenced to the COSPAR profiles) taken directly from the Viking scenario GCM run at $L_S = 0°$, $L_S = 90°$, $L_S = 180°$ and $L_S = 270°$. The variability model simulations of these fields are shown in Figure 12. On a large scale the variability model captures the seasonal cycle of density variability well. Small differences between the GCM and the variability model simulated fields are due to the random nature of the PC model (Equation 21).

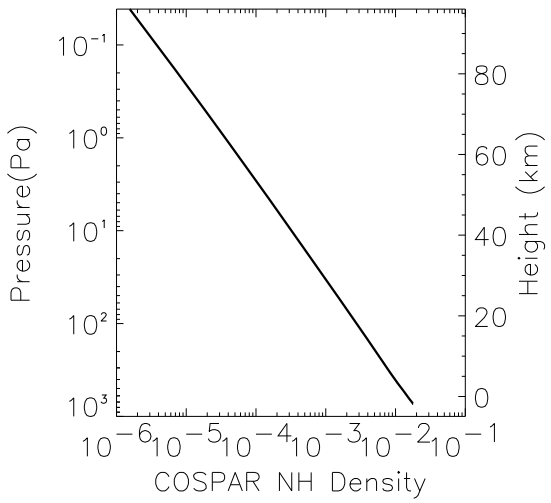

Figure 10: COSPAR northern hemisphere mean density ($\mathrm{kg\,m^{-3}}$) for Mars. Note the logarithmic scale on the abscissa.

5.2 The Small-Scale Variability Model

The small-scale variability model simulates perturbations of density, temperature and wind due to the upward propagation of small-scale gravity waves. The model is based on the parameterization scheme used in the numerical models that simulated the data in the database (see Collins *et. al*, 1997).

The surface stress exerted by a vertically-propagating, stationary gravity wave can be written

$$\tau_0 \;=\; \kappa\rho_0 N_0 |\mathbf{v_0}| \sigma_0 \tag{23}$$

where κ is a characteristic gravity wave horizontal wave number, ρ_0 is the surface density, N_0 is the surface Brunt Väisälä frequency, $\mathbf{v_0}$ is the surface vector wind and σ_0 is a measure of the orographic variance. In this case we choose the model sub-grid scale orographic variance. The surface stress can be related to the gravity wave vertical isentropic displacement, δh, by

$$\tau_0 \;=\; \kappa\rho_0 N_0 |\mathbf{v_0}| \delta h^2 . \tag{24}$$

We then assume that the stress, τ, above the surface is equal to that at the surface. This leads to an expression for δh, at height z,

$$\delta h \;=\; \sqrt{\frac{\rho_0 N_0 |\mathbf{v_0}| \sigma_0}{\rho N |\mathbf{v}|}} \tag{25}$$

where ρ, N and $\mathbf{v}$ are the density, Brunt Väisälä frequency and vector wind at height z.

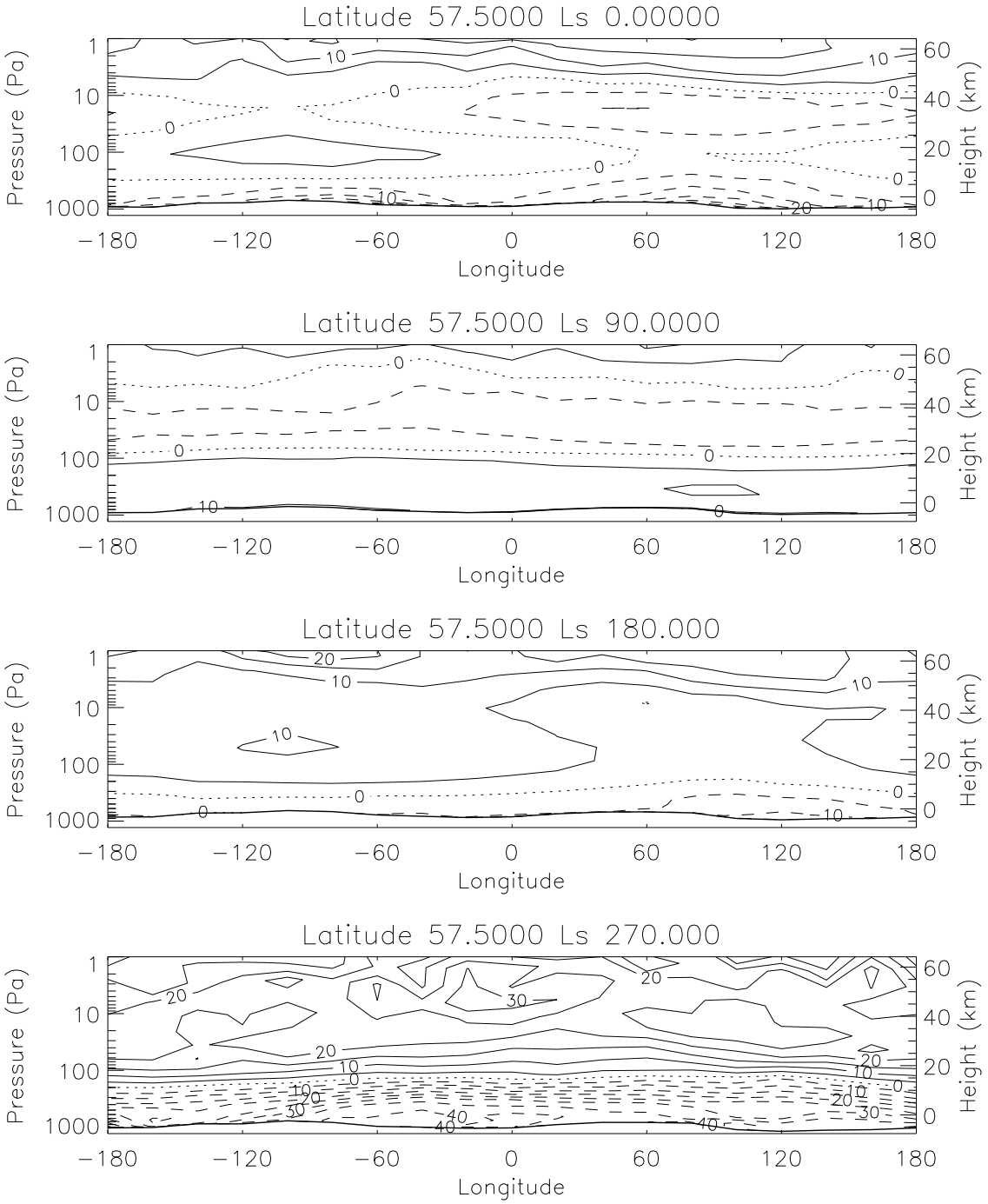

Figure 11: Longitude-height cross sections of density at 57.5°N expressed as a deviation from the COSPAR northern hemisphere reference profile at several seasonal dates. The fields are instantaneous and have been taken from the Viking scenario GCM run.

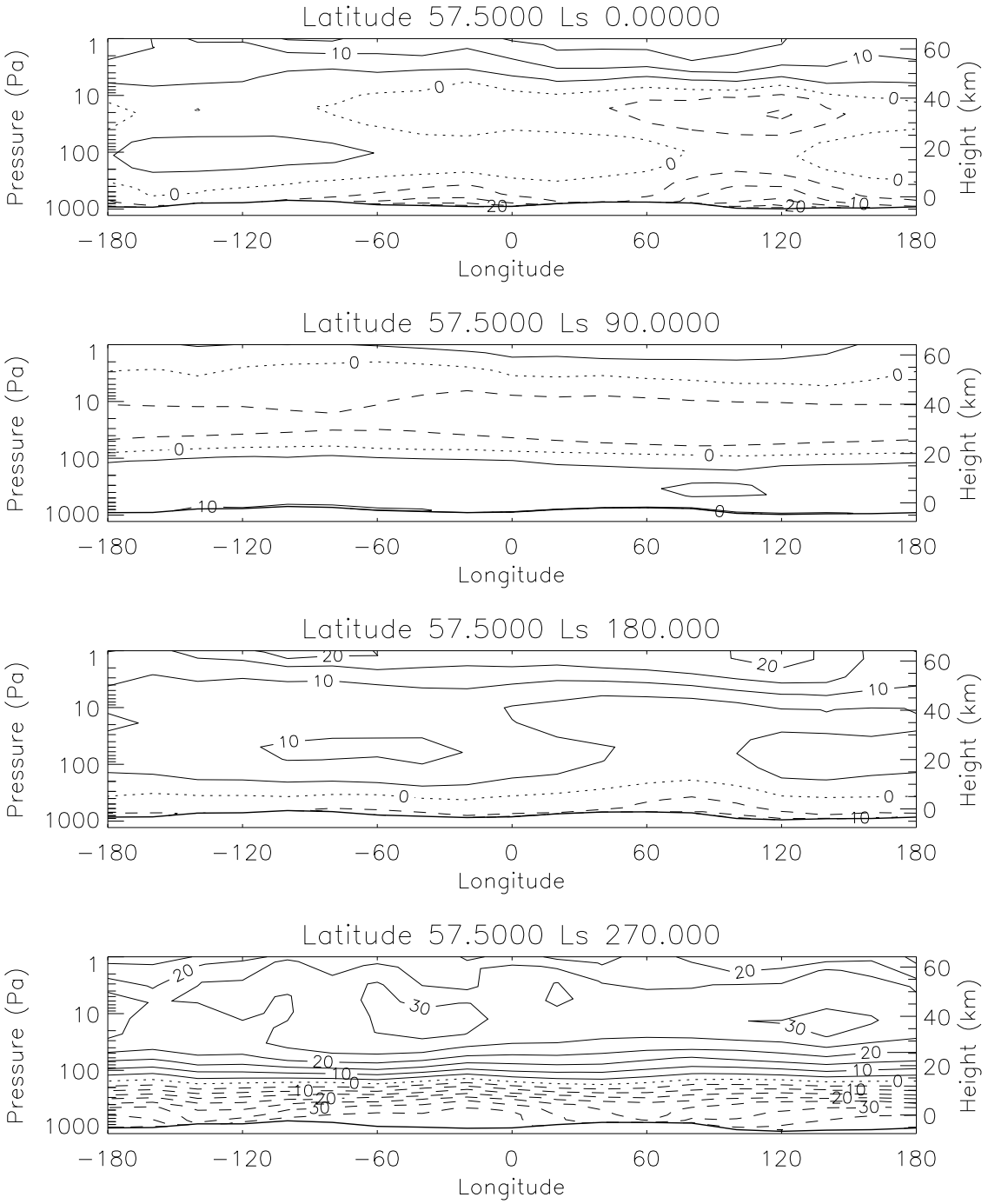

Figure 12: Longitude-height cross sections of density at 57.5°N simulated using the new variability model and expressed as a deviation from the COSPAR northern hemisphere reference profile.

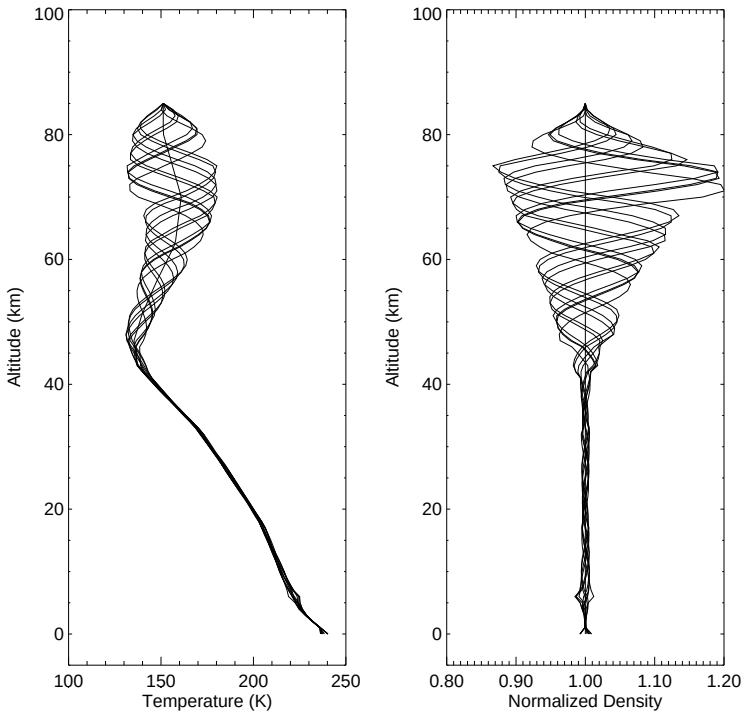

Figure 13: A series of ten perturbations generated by the small scale variability model added to mean profiles of temperature and density from the MCD; these correspond to the Viking Lander 1 entry location and time.

The gravity wave perturbation to a meteorological variable is calculated by considering vertical displacements of the form

$$\delta z = \delta h \sin\left(\frac{2\pi z}{\lambda} + \phi_0\right) \tag{26}$$

where λ is a characteristic vertical wavelength for the gravity wave and ϕ_0 is a randomly generated surface phase angle. Perturbations to temperature, density and wind at height z are then found by using the value at $z + \delta z$ on the background profile, with the perturbations to temperature and density calculated on the assumption of adiabatic motion to the valid height. A value can be chosen for λ to provide a reasonable comparison with the observed Viking entry temperature profiles above 50 km; we take $\lambda = 16$ km. An example of several small scale perturbations is shown in Figure 13.

6 References

Collins, M. and Lewis, S.R. (1997) *Mars Climate Database v1.0: User Manual,* European Space Agency Technical Report.

Collins, M. and Lewis, S.R. (1997) *Mars Climate Database v1.0: Detailed Design Document,* European Space Agency Technical Report.

Collins, M., Lewis, S.R., Read, P.L., Thomas, N.P.J., Talagrand, O., Forget, F., Fournier, R., Hourdin, F. and Huot, J.-P. (1996) "A climate database for the Martian atmosphere," in *Environment Modelling for Space-based Applications,* European Space Agency **SP–392,** 323–327.

Collins, M., Lewis, S.R. and Read, P.L. (1997) "Gravity wave drag in a global circulation model of the Martian atmosphere: Parameterisation and validation," *Adv. Space Res.,* **19,** 1245–1254.

Forget, F., Hourdin, F., Fournier, R., Hourdin, C., Talagrand, O., Collins, M., Lewis, S.R., Read, P.L. and Huot, J.-P. (1999) "Improved general circulation models of the Martian atmosphere from the surface to above 80 km," *J. Geophys. Res.,* **104,** 24,155–24,176.

Forget, F., C. Hourtolle, and Lewis, S.R. (2000a) *Mars Climate Database atmemcd subroutine prgrammer's guide.*

Hourtolle, C., Forget, F. and Lewis, S.R. (2000b) *Mars Climate Database "atmemcd" subroutine programmer's reference.*

Justus, C.G. (1990) "A Mars Global Reference Atmosphere Model (Mars-GRAM) for mission planning and analysis," *AIAA Paper No. 90–0004,* 28th Aerospace Sciences Meeting.

Justus, C.G., Alyea, F.N., Cunnold, D.M., Jeffries, W.R. III, and Johnson, D.L. (1995) "The NASA/MSFC Global Reference Atmosphere Model – 1995 Version (GRAM-95)," *NASA Technical Memorandum.*

Lewis, S.R. and Collins, M. (1999a) *Mars Climate Database v2.0: User Manual,* European Space Agency Technical Report.

Lewis, S.R. and Collins, M. (1999b) *Mars Climate Database v2.0: Detailed Design Document,* European Space Agency Technical Report.

Lewis, S.R., Collins, M. and Forget, F. (2000a) *Mars Climate Database v2.3: User Manual,* European Space Agency Technical Report.

Lewis, S.R., Collins, M. and Forget, F. (2000b) *Mars Climate Database v2.3: Detailed Design Document,* European Space Agency Technical Report.

Lewis, S.R., Collins, M., Read, P.L., Forget, F., Hourdin, F., Fournier, R., Hourdin, C., Talagrand, O. and Huot, J.-P. (1999) "A Climate Database for Mars," *J. Geophys. Res.,* **104,** 24,177–24,194.

Mo, K.C., and Ghil, M. (1987) “Statistics and dynamics of persistent anomalies,” *J. Atmos. Sci.,* **55,** 877–901.

North, G.R. (1984) “Empirical Orthogonal Functions and Normal Modes,” *J. Atmos. Sci.* **41,** 879–887.

Read, P.L., Collins, M., Forget, F., Fournier, R., Hourdin, F., Lewis, S.R., Talagrand, O., Taylor, F.W. and Thomas, N.P.J. (1997) “A GCM climate database for Mars: For mission planning and for scientific studies,” *Adv. Space Res.* **19,** 1213–1222.